Chapter 9
Electron and Phonon Scattering

9.1 Electron Scattering

The thermal properties of solid materials depend on the availability of carriers and on their scattering rates. In the previous chapters, we focused on the carriers and their generation. In this Chapter we focus on the relevant electron and phonon scattering mechanisms.

Electron scattering brings an electronic system which has been subjected to external perturbations back to equilibrium. Collisions also alter the momentum of all the carriers, as the electrons are brought back into equilibrium. Electron collisions can occur through a variety of mechanisms, such as electron-phonon, electron-impurity, electron-defect, electron-boundary and electron-electron scattering processes. Electron scattering is handled here by considering the collision term in the Boltzmann equation.

In principle, the collision rates can be calculated from using scattering theory in single form. To do this, we introduce a transition probability $S(\mathbf{k}, \mathbf{k}')$ for scattering the electron from a state $\mathbf{k}$ to a state $\mathbf{k}'$. Since electrons obey the Pauli principle, scattering will occur from an occupied to an unoccupied state. The process of scattering from $\mathbf{k}$ to $\mathbf{k}'$ decreases the distribution function $f(\mathbf{r}, \mathbf{k}, t)$ depending on the probability that $\mathbf{k}$ is occupied and that $\mathbf{k}'$ is unoccupied. The process of scattering an electron from $\mathbf{k}'$ to $\mathbf{k}$ increases the distribution function $f(\mathbf{r}, \mathbf{k}, t)$ and depends on the probability that state $\mathbf{k}'$ is occupied and state $\mathbf{k}$ is unoccupied. We will use the following notation for describing a general scattering process:

- f_k is the probability that an electron occupied with initial state $\mathbf{k}$
- $[1 - f_k]$ is the probability that state $\mathbf{k}$ is unoccupied
- $S(\mathbf{k}, \mathbf{k}')$ is the probability per unit time that an electron in state $\mathbf{k}$ will be scattered to state $\mathbf{k}'$
- $S(\mathbf{k}', \mathbf{k})$ is the probability per unit time that an electron in state $\mathbf{k}'$ will be scattered back into state $\mathbf{k}$.

M. Dresselhaus et al., *Solid State Properties*, Graduate Texts in Physics,
https://doi.org/10.1007/978-3-662-55922-2_9

Using these definitions, the rate of change of the distribution function in the Boltzmann equation (see (7.4)) due to collisions can be written as:

$$\left.\frac{\partial f(\mathbf{r},\mathbf{k},t)}{\partial t}\right|_{\text{collisions}} = \int d^3k'[f_{k'}(1-f_k)S(\mathbf{k}',\mathbf{k}) - f_k(1-f_{k'})S(\mathbf{k},\mathbf{k}')] \quad (9.1)$$

where d^3k' is a volume element in $\mathbf{k}'$ space. The integration in (9.1) is over k space and the spherical coordinate system is shown in Fig. 9.1, together with the arbitrary force $\mathbf{F}$ responsible for the scattering event that introduces a perturbation described by

$$f_{\mathbf{k}} = f_{0\mathbf{k}} + \frac{\partial f_{0\mathbf{k}}}{\partial E}\frac{\hbar}{m^*}\mathbf{k}\cdot\mathbf{F} + \ldots \quad (9.2)$$

where $f_{0\mathbf{k}}$ denotes the equilibrium distribution. Using Fermi's Golden Rule for the transition probability per unit time between states $\mathbf{k}$ and $\mathbf{k}'$ we can write

$$S(\mathbf{k},\mathbf{k}') \simeq \frac{2\pi}{\hbar}|\mathscr{H}_{\mathbf{k}\mathbf{k}'}|^2\{\delta[E(\mathbf{k})] - \delta[E(\mathbf{k}')]\} \quad (9.3)$$

where the matrix element of the Hamiltonian coupling states $\mathbf{k}$ and $\mathbf{k}'$ is

$$\mathscr{H}_{\mathbf{k}\mathbf{k}'} = \frac{1}{N}\int_V \psi^*_{\mathbf{k}}(\mathbf{r})\nabla V\psi_{\mathbf{k}'}(\mathbf{r})d^3r, \quad (9.4)$$

in which N is the number of unit cells in the sample and ∇V is the perturbation Hamiltonian term responsible for the scattering event associated with the force $\mathbf{F}$.

At equilibrium $f_k = f_0(E)$ and the principle of detailed balance applies

$$S(\mathbf{k}',\mathbf{k})f_0(E')[1-f_0(E)] = S(\mathbf{k},\mathbf{k}')f_0(E)[1-f_0(E')] \quad (9.5)$$

so that the distribution function does not experience a net change via collisions when in the equilibrium state:

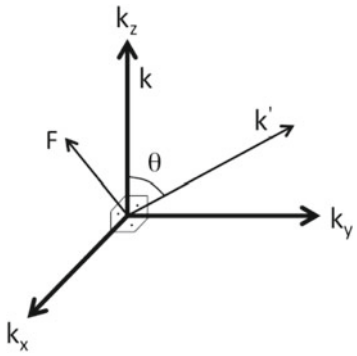

Fig. 9.1 Coordinate system in reciprocal space for an electron with wave vector $\mathbf{k}$ (along the k_z axis) scattering into a state with wavevector $\mathbf{k}'$ in an arbitrary force field $\mathbf{F}$. The scattering center is at the origin of the coordinate system. For simplicity the event is rotated so that $\mathbf{F}$ has no k_y component

$$(\partial f(\mathbf{r}, \mathbf{k}, t)/\partial t)|_{\text{collisions}} = 0. \tag{9.6}$$

We define collisions as *elastic collisions* when $E(\mathbf{k}') = E(\mathbf{k})$ and in this case $f_0(E') = f_0(E)$ so that $S(\mathbf{k}', \mathbf{k}) = S(\mathbf{k}, \mathbf{k}')$. Collisions for which $E(\mathbf{k}') \neq E(\mathbf{k})$ are termed *inelastic* collisions. The term *quasi-elastic* is used to characterize collisions where the percentage change in energy is small. For our purposes here, we shall consider $S(\mathbf{k}, \mathbf{k}')$ as a known function which can be calculated quantum mechanically by a detailed consideration of the scattering mechanisms which are important for a given practical case; this statement is true in principle, but in practice $S(\mathbf{k}, \mathbf{k}')$ is usually specified in an approximate way.

The return to equilibrium depends on the frequency of collisions and the effectiveness of a scattering event in randomizing the motion of the electrons. Thus, small angle scattering is not as effective in restoring a system to equilibrium as for the case of large angle scattering. For this reason we distinguish between τ_D, the time for the system to be restored to equilibrium, and τ_c, the time between collisions. These times are related by

$$\tau_D = \frac{\tau_c}{1 - \cos\theta} \tag{9.7}$$

where θ is the mean change of angle of the electron velocity on collision (see Fig. 9.1). The time τ_D is the quantity which enters into Boltzmann's equation as the relaxation time, while $1/\tau_c$ determines the actual scattering rate.

The mean free time between collisions, τ_c, is related to several other quantities of interest: the mean free path ℓ_f, the scattering cross section σ_d, and the concentration of scattering centers N_c by

$$\tau_c = \frac{1}{N_c \sigma_d v} \tag{9.8}$$

where v is the drift velocity given by

$$v = \frac{\ell_f}{\tau_c} = \frac{1}{N_c \sigma_d \tau_c} \tag{9.9}$$

and v is in the direction of the electron transport. From (9.9), we see that $\ell_f = 1/N_c\sigma_d$. The drift velocity is of course very much smaller in magnitude than the instantaneous velocity of the electron at the Fermi level, which is typically of magnitude $v_F \sim 10^8$ cm/s. Electron scattering centers include phonons, impurities, dislocations, vacancies, the crystal surface, etc.

The most important electron scattering mechanism for both metals and semiconductors is electron-phonon scattering (scattering of electrons by the thermal motion of the lattice), though the scattering processes for metals differs in detail from those in semiconductors. In the case of metals, much of the Brillouin zone is occupied by electrons, while in the case of semiconductors, most of the Brillouin zone is unoccupied, and represents states into which electrons can be scattered. In the case of metals, electrons are scattered from one point on the Fermi surface to another point on the Fermi surface, and a large change in momentum occurs, corresponding to a

large change in **k**. In the case of semiconductors, changes in wave vector from **k** to −**k** normally correspond to a very small change in wave vector, and thus changes from **k** to −**k** can be accomplished much more easily in the case of semiconductors. By the same token, small angle scattering (which is not so efficient for returning the system to equilibrium) is especially important for semiconductors where the change in wavevector is small. Since the scattering processes in semiconductors and metals are quite different, they will be discussed separately in the next sections.

Scattering probabilities for more than one scattering process are taken to be additive and therefore so are the reciprocal scattering times and scattering rates. For the total reciprocal scattering time $(\tau^{-1})_{\text{total}}$ we write:

$$(\tau^{-1})_{\text{total}} = \sum_i \tau_i^{-1} \tag{9.10}$$

since $1/\tau$ is proportional to the scattering probability. Equation (9.10) is commonly referred to as "Matthiessen's rule" Metals have large Fermi wavevectors k_F, and therefore large momentum transfers Δk can occur as a result of electronic collisions. In contrast, for semiconductors, k_F is small and so also is Δk on collision.

9.2 Scattering Processes in Semiconductors

9.2.1 Electron-Phonon Scattering in Semiconductors

Electron-phonon scattering is the dominant scattering mechanism in crystalline semiconductors except at very low temperatures where the phonon density is low. Conservation of energy in the scattering process, which creates or absorbs a phonon of energy $\hbar\omega(\mathbf{q})$, is written as:

$$E_i - E_f = \pm\hbar\omega(\mathbf{q}) = \frac{\hbar^2}{2m^*}(k_i^2 - k_f^2), \tag{9.11}$$

where E_i is the initial energy, E_f is the final energy, k_i the initial wavevector, and k_f the final wavevector. Here, the "+" sign corresponds to the creation of phonons (the phonon emission process), while the "−" sign corresponds to the annihilation of phonons (the phonon absorption process). Conservation of momentum in the scattering of an electron by a phonon of wavevector **q** yields

$$\mathbf{k_i} - \mathbf{k_f} = \pm\mathbf{q}. \tag{9.12}$$

For semiconductors, the electrons involved in the scattering event generally remain in the vicinity of a single band extremum and involve only a small change in **k** and hence only low phonon **q** vectors participate. The probability that an electron makes a transition from an initial state i to a final state f is proportional to:

(a) the availability of final states for electrons,
(b) the probability of absorbing or emitting a phonon,
(c) the strength of the electron-phonon coupling or electron-phonon interaction.

The first factor, the availability of final states, is proportional to the density of final electron states $\rho(E_f)$ times the probability that the final state is unoccupied. This occupation probability for a semiconductor is assumed to be unity since the conduction band is essentially empty. For a simple parabolic band, $\rho(E_f)$ is (from (7.64)):

$$\rho(E_f) = \frac{(2m^*)^{3/2} E_f^{1/2}}{2\pi^2\hbar^3} = (2m^*)^{3/2} \frac{[E_i \pm \hbar\omega(\mathbf{q})]^{1/2}}{2\pi^2\hbar^3}, \tag{9.13}$$

where (9.11) has been employed and the "+" sign corresponds to absorption of a phonon and the "−" sign corresponds to phonon emission.

The probability of absorbing or emitting a phonon is proportional to the electron-phonon coupling $G(\mathbf{q})$ and to the phonon density $n(\mathbf{q})$ for absorption, and the phonon density $[1 + n(\mathbf{q})]$ for emission, where $n(\mathbf{q})$ is given by the Bose-Einstein factor

$$n(\mathbf{q}) = \frac{1}{e^{\hbar\omega(\mathbf{q})/k_B T} - 1}. \tag{9.14}$$

Combining the terms in (9.13) and (9.14) gives a scattering probability (or $1/\tau_c$) proportional to a sum over final states

$$\frac{1}{\tau_c} \sim \frac{(2m^*)^{3/2}}{2\pi^2\hbar^3} \sum_{\mathbf{q}} G(\mathbf{q}) \left[\frac{[E_i + \hbar\omega(\mathbf{q})]^{1/2}}{e^{\hbar\omega(\mathbf{q})/k_B T} - 1} + \frac{[E_i - \hbar\omega(\mathbf{q})]^{1/2}}{1 - e^{-\hbar\omega(\mathbf{q})/k_B T}} \right] \tag{9.15}$$

where the first term in the big bracket of (9.15) corresponds to phonon absorption and the second term to phonon emission. If $E_i < \hbar\omega(\mathbf{q})$, only the *phonon absorption* process is energetically allowed.

The electron-phonon coupling coefficient $G(\mathbf{q})$ in (9.15) depends on the electron-phonon coupling mechanism. There are three important coupling mechanisms in semiconductors which we briefly describe below: electromagnetic coupling, piezoelectric coupling, and deformation-potential coupling.

Electromagnetic Coupling

This coupling is important only for semiconductors where the charge distribution has different signs on neighboring ion sites when two species of atoms are involved. In this case, the oscillatory electric field can give rise to oscillating dipole moments associated with the motion of neighboring ion sites in the optical modes (see Fig. 9.2). The electromagnetic coupling mechanism is important in coupling electrons to optical phonon modes in III-V and II-VI compound semiconductors, but does not contribute in the case of silicon. To describe the optical modes we can use the Einstein approxi-

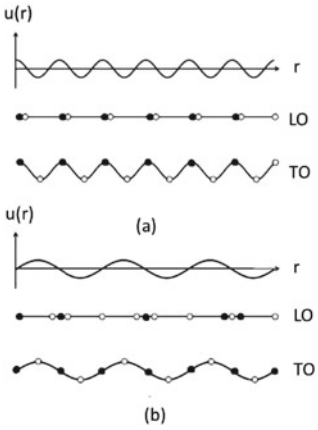

Fig. 9.2 Displacements $\mathbf{u}(\mathbf{r})$ of atoms in a diatomic chain for longitudinal optical (LO) and transverse optical (TO) phonons at **a** the center and **b** the edge of the Brillouin zone. The lighter mass atoms are indicated by open circles. For zone edge optical phonons, only the lighter atoms are displaced

mation, since $\omega(\mathbf{q})$ is only weakly dependent on $\mathbf{q}$ for the optical modes of frequency ω_0. In this case $\hbar\omega_0 \gg k_B T$ and $\hbar\omega_0 \gg E$ where E is the electron energy, so that from (9.15) the collision rate is proportional to

$$\frac{1}{\tau_c} \sim \frac{m^{*3/2}(\hbar\omega_0)^{1/2}}{e^{\hbar\omega_0/k_B T} - 1}. \tag{9.16}$$

Thus, the collision rate depends on the temperature T, the optical phonon frequency ω_0 and the electron effective mass m^*. The corresponding mobility for *optical phonon scattering* is

$$\mu = \frac{e\langle\tau\rangle}{m^*} \sim \frac{e(e^{\hbar\omega_0/k_B T} - 1)}{m^{*5/2}(\hbar\omega_0)^{1/2}} \tag{9.17}$$

Thus for optical phonon scattering, the mobility μ is independent of the electron energy E and decreases with increasing temperature.

Piezoelectric Coupling

As in the case of electromagnetic coupling, piezoelectric coupling is important in semiconductors which are ionic or partly ionic. If these crystals lack inversion symmetry, then *acoustic* mode vibrations generate regions of compression and rarefaction in a crystal which in here lead to the generation of electric fields (see Fig. 9.3). The piezoelectric scattering mechanism is thus associated with the coupling between electrons and phonons arising from these electromagnetic fields. The zincblende structure of the III–V compounds (e.g., GaAs) lacks inversion symmetry. In this case the perturbation potential is given by

$$\Delta V(\mathbf{r}, t) = \frac{-ie\varepsilon_{pz}}{\varepsilon_0 q} \nabla \cdot \mathbf{u}(\mathbf{r}, t) \tag{9.18}$$

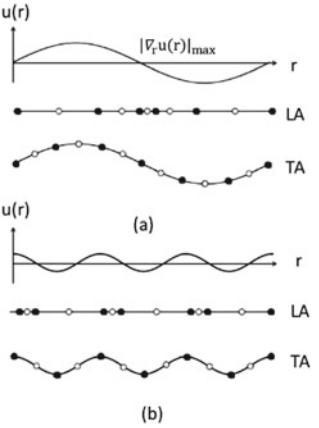

Fig. 9.3 Displacements $\mathbf{u}(\mathbf{r})$ of atoms on a diatomic chain for longitudinal acoustic (LA) and transverse acoustic (TA) phonons at **a** the center and **b** the edge of the Brillouin zone. The lighter mass atoms are indicated by open circles. For zone edge acoustic phonons, only the heavier atoms are displaced

where ε_{pz} is the piezoelectric coefficient and $\mathbf{u}(\mathbf{r}, t) = u \exp(i\mathbf{q} \cdot \mathbf{r} - \omega t)$ is the displacement during a normal mode oscillation. Note that the phase of $\Delta V(\mathbf{r}, t)$ in piezoelectric coupling is shifted by $\pi/2$ relative to the case of electromagnetic coupling.

Deformation-Potential Coupling

The deformation-potential coupling mechanism is associated with energy shifts of the energy band extrema caused by the compression and rarefaction of crystals during acoustic mode vibrations. The deformation potential scattering mechanism is important in crystals like silicon which have inversion symmetry (and hence no piezoelectric scattering coupling) and have the same species on each site (and hence no electromagnetic coupling). The longitudinal acoustic modes are important for phonon coupling in n-type Si and Ge where the conduction band minima occur away from $\mathbf{k} = 0$.

For deformation potential coupling, it is the LA acoustical phonons that are most important, though contributions by LO optical phonons still make some contribution. For the acoustic phonons, we have the condition $\hbar\omega \ll k_B T$ and $\hbar\omega \ll E$, while for the optical phonons it is usually the case that $\hbar\omega \gg k_B T$ at room temperature. For the range of acoustic phonon modes of interest, $G(\mathbf{q}) \sim q$, where q is the phonon wave vector and $\omega \sim q$ for acoustic phonons. Furthermore for the LA phonon branch, the phonon absorption process will depend on $n(q)$ in accordance with the Bose factor

$$\frac{1}{e^{\hbar\omega/k_B T} - 1} \simeq \frac{1}{\left[1 + \frac{\hbar\omega}{k_B T} + \cdots\right] - 1} \sim \frac{k_B T}{\hbar\omega} \sim \frac{k_B T}{q}, \tag{9.19}$$

while for phonon emission

$$\frac{1}{1 - e^{-\hbar\omega/k_B T}} \simeq \frac{1}{1 - \left[1 - \frac{\hbar\omega}{k_B T} + \cdots\right]} \sim \frac{k_B T}{\hbar\omega} \sim \frac{k_B T}{q}. \tag{9.20}$$

Therefore, in considering both phonon absorption and phonon emission, the respective factors

$$G(\mathbf{q})[e^{\hbar\omega/k_BT} - 1]^{-1}$$

and

$$G(\mathbf{q})[1 - e^{-\hbar\omega/k_BT}]^{-1}$$

are both independent of q for the LA branch. Consequently for the *acoustic phonon scattering* process, the carrier mobility μ decreases with increasing T according to (see (9.15))

$$\mu = \frac{e\langle\tau\rangle}{m^*} \sim m^{*-5/2}E^{-1/2}(k_BT)^{-1}. \tag{9.21}$$

For the optical LO contribution, we have a $G(\mathbf{q})$ independent of $\mathbf{q}$ but an $E^{1/2}$ factor is introduced by (9.15) for both phonon absorption and emission, leading to the same basic dependence as given by (9.21). Thus, we find that the temperature and energy dependence of the mobility μ is different for the various electron-phonon coupling mechanisms. These differences in the E and T dependences can thus be used to identify which scattering mechanism is dominant in specific semiconducting samples. Furthermore, when explicit account is taken of the energy dependence of τ, then departures from the strict Drude model $\sigma = ne^2\tau/m^*$ can be expected.

9.2.2 *Ionized Impurity Scattering*

As the temperature is reduced, phonon scattering becomes less important so that in this regime, ionized impurity scattering and other defect scattering mechanisms can become dominant. Ionized impurity scattering can also be important in heavily doped semiconductors over a wider temperature range because of the larger defect density. This scattering mechanism involves the deflection of an electron with velocity v by the Coulomb field of an ion with charge Ze, as modified by the dielectric constant ε of the medium and by the screening of the impurity ion by free electrons (see Fig. 9.4). Most electrons are scattered through small angles as they are scattered by ionized impurities. The perturbation potential is given by

$$\Delta V(\mathbf{r}) = \frac{\pm Ze^2}{4\pi\varepsilon_0 r} \tag{9.22}$$

and the $\pm$ signs denote the different scattering trajectories for electrons and holes (see Fig. 9.4). In (9.22) the screening of the electron by the semiconductor environment is handled by the static dielectric constant of the semiconductor ε_0. Because of the long-range nature of the Coulomb interaction, screening by other free carriers and by other ionized impurities could be important. Such screening effects are further discussed in Sect. 9.2.4.

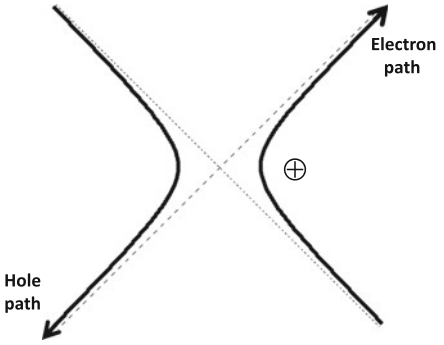

Fig. 9.4 Trajectories of electrons and holes in ionized impurity scattering. The scattering center is at the origin

The scattering rate $1/\tau_I$ due to ionized impurity scattering is given to a good approximation by the Conwell–Weisskopf formula

$$\frac{1}{\tau_I} \sim \frac{Z^2 N_I}{m^{*1/2} E^{3/2}} \ell n \left\{ 1 + \left[\frac{4\pi\varepsilon E}{Z e^2 N_I^{1/3}} \right]^2 \right\} \tag{9.23}$$

in which N_I is the ionized charged impurity density. The Conwell–Weisskopf formula works quite well for heavily doped semiconductors. We note here that $\tau_I \sim E^{3/2}$, so that it is the low energy electrons that are most affected by ionized impurity scattering (see Fig. 7.10).

Neutral impurities also introduce a scattering potential, but it is much weaker than that for the ionized impurity. Free carriers can polarize a neutral impurity and interact with the resulting dipole moment, or can undergo an exchange interaction. In the case of neutral impurity scattering, the perturbation potential is given by

$$\Delta V(\mathbf{r}) \simeq \frac{\hbar^2}{m^*} \left(\frac{r_B}{r^5} \right)^{1/2} \tag{9.24}$$

where r_B is the ground state Bohr radius of the electron in a doped semiconductor and r is the distance of the electron to the neutral impurity scattering center.

9.2.3 Other Scattering Mechanisms

Other scattering mechanisms in semiconductors include:

(a) neutral impurity centers — these make contributions at very low temperatures, and are mentioned in Sect. 9.2.2. Neutral impurity centers can also cause local strain effects which scatter carriers.

(b) dislocations — these defects give rise to anisotropic scattering at low temperatures.
(c) boundary scattering by crystal surfaces — this scattering becomes increasingly important, the smaller the crystal size. Boundary scattering can become a dominant scattering mechanism in nanostructures (e.g., quantum wells, quantum wires and quantum dots), when the sample size in the confinement direction is smaller that the bulk mean free path. These electrons do not reach equilibrium and are therefore called ballistic electrons (or holes).
(d) intervalley scattering from one equivalent conduction band minimum to another. This scattering process requires a phonon with large q and consequently results in a relatively large energy transfer.
(e) electron-electron scattering – similar to charged impurity scattering in being dominated by a Coulomb scattering mechanism, except that spin effects become important for spin–spin scattering. This mechanism can be important in distributing energy and momentum among the electrons in the solid and thus can act in conjunction with other scattering mechanisms in establishing equilibrium.
(f) electron-hole scattering — depends on having both electrons and holes present. Because the electron and hole motions induced by an applied electric field are in opposite directions, electron-hole scattering tends to reverse the direction of the incident electrons and holes. Radiative recombination, i.e., electron-hole recombination with the emission of a photon, must also be considered.
(g) ballistic carriers — charge carriers passing through sample without scattering and not coming to equilibrium with the lattice.

9.2.4 Screening Effects in Semiconductors

In the vicinity of a charged impurity or an acoustic phonon, charge carriers are accumulated or depleted by the scattering potential, giving rise to a charge density

$$\rho(\mathbf{r}) = e[n(\mathbf{r}) - p(\mathbf{r}) + N_a^-(\mathbf{r}) - N_d^+(\mathbf{r})] = en^*(\mathbf{r}) \tag{9.25}$$

where $n(\mathbf{r})$, $p(\mathbf{r})$, $N_a^-(\mathbf{r})$, $N_d^+(\mathbf{r})$, and $n^*(\mathbf{r})$ are, respectively, the electron, hole, ionized acceptor, ionized donor, and effective total carrier concentrations as a function of distance r to the scatterer. We can then write expressions for these quantities in terms of their excess charge above the uniform potential in the absence of the charge perturbation

$$\begin{aligned} n(\mathbf{r}) &= n + \delta n(\mathbf{r}) \\ N_d^+(\mathbf{r}) &= N_d^+ + \delta N_d^+(\mathbf{r}), \end{aligned} \tag{9.26}$$

and similarly for the holes and acceptors. The space charge $\rho(\mathbf{r})$ is related to the perturbing potential by Poisson's equation

$$\nabla^2\phi(\mathbf{r}) = -\frac{\rho(\mathbf{r})}{\varepsilon_0}. \tag{9.27}$$

Approximate relations for the excess concentrations are

$$\begin{aligned} \delta n(\mathbf{r})/n &\simeq -e\phi(\mathbf{r})/(k_B T) \\ \delta N_d^+(\mathbf{r})/N_d^+ &\simeq e\phi(\mathbf{r})/(k_B T) \end{aligned} \tag{9.28}$$

and similar relations for the holes. Substitution of (9.25) into (9.26) and (9.28) yield

$$\nabla^2\phi(\mathbf{r}) = -\frac{n^* e^2}{\varepsilon_0 k_B T}\phi(\mathbf{r}). \tag{9.29}$$

We define an effective Debye screening length λ such that

$$\lambda^2 = \frac{\varepsilon_0 k_B T}{n^* e^2}. \tag{9.30}$$

For a spherically symmetric potential (9.29) becomes

$$\frac{d^2}{dr^2}\Big(r\phi(r)\Big) = \frac{r\phi(r)}{\lambda^2} \tag{9.31}$$

which yields a solution

$$\phi(r) = \frac{Ze^2}{4\pi\varepsilon_0 r}e^{-r/\lambda}. \tag{9.32}$$

Thus, the screening effect produces an exponential decay of the scattering potential $\phi(r)$ with a characteristic length λ that depends through (9.30) on the effective electron concentration. When the concentration gets large, λ decreases and screening becomes more effective.

When applying screening effects to the ionized impurity scattering problem, we Fourier expand the scattering potential to take advantage of the overall periodicity of the lattice

$$\Delta V(\mathbf{r}) = \sum_G A_G \exp(i\mathbf{G}\cdot\mathbf{r}) \tag{9.33}$$

where the Fourier coefficients are given by

$$A_G = \frac{1}{V}\int_V \nabla V(\mathbf{r})\exp(-i\mathbf{G}\cdot\mathbf{r})d^3r \tag{9.34}$$

and the matrix element of the perturbation Hamiltonian in (9.4) becomes

$$\mathscr{H}_{\mathbf{k},\mathbf{k}'} = \frac{1}{N}\sum_G \int_V e^{-i\mathbf{k}\cdot\mathbf{r}} u_k^*(r) A_G e^{-i\mathbf{G}\cdot\mathbf{r}} e^{i\mathbf{k}'\cdot\mathbf{r}} u_{k'}(r) d^3r. \tag{9.35}$$

We note that the integral in (9.35) vanishes unless $\mathbf{k} - \mathbf{k}' = \mathbf{G}$ so that

$$\mathscr{H}_{\mathbf{k},\mathbf{k}'} = \frac{A_G}{N}\int_V u_k^*(r) u_{k'}(r) d^3r \tag{9.36}$$

within the first Brillouin zone so that for parabolic bands $u_k(\mathbf{r}) = u_{k'}(\mathbf{r})$ and

$$\mathscr{H}_{\mathbf{k},\mathbf{k}'} = A_{\mathbf{k}-\mathbf{k}'}. \tag{9.37}$$

Now substituting for the scattering potential in (9.34) we obtain

$$A_G = \frac{Ze^2}{4\pi\varepsilon_0 V}\int_V \exp(-i\mathbf{G}\cdot\mathbf{r}) d^3r \tag{9.38}$$

where $d^3r = r^2 \sin\theta d\theta d\phi dr$ so that, for $\phi(r)$ depending only on r, the angular integration gives 4π and the spatial integration gives

$$A_G = \frac{Ze^2}{\varepsilon_0 V|\mathbf{G}|^2} \tag{9.39}$$

and

$$\mathscr{H}_{\mathbf{k},\mathbf{k}'} = \frac{Ze^2}{\varepsilon_0 V|\mathbf{k}-\mathbf{k}'|^2}. \tag{9.40}$$

Equations (9.39) and (9.40) are valid for the scattering potential without screening. When screening is included in considering the ionized impurity scattering mechanism, the integration becomes

$$A_G = \frac{Ze^2}{4\pi\varepsilon_0 V}\int_V e^{-r/\lambda} e^{-i\mathbf{G}\cdot\mathbf{r}} d^3r = \frac{Ze^2}{\varepsilon_0 V[|\mathbf{G}|^2 + |1/\lambda|^2]} \tag{9.41}$$

and

$$\mathscr{H}_{\mathbf{k},\mathbf{k}'} = \frac{Ze^2}{\varepsilon_0 V[|\mathbf{k}-\mathbf{k}'|^2 + |1/\lambda|^2]} \tag{9.42}$$

so that screening clearly reduces the scattering due to ionized impurity scattering. The discussion given here also extends to the case of scattering in metals, which is treated below.

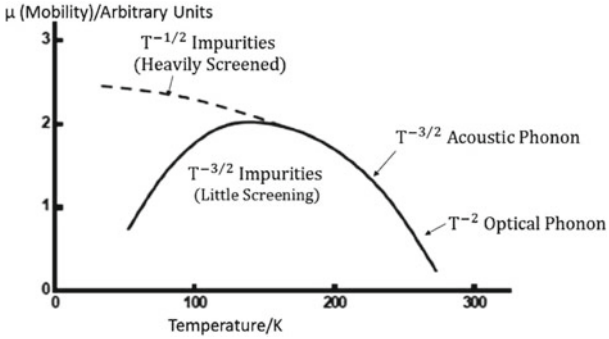

Fig. 9.5 Typical temperature dependence of the carrier mobility in semiconductors, showing the effect of the dominant scattering mechanisms and the temperature dependence of each

Combining the various scattering mechanisms discussed above for semiconductors, the picture given by Fig. 9.5 emerges. Here we see the temperature dependence of each of the important scattering mechanisms and the effect of each of these processes on the carrier mobility. Here it is seen that screening effects are important for carrier mobilities at low temperature.

9.3 Electron Scattering in Metals

Basically the same scattering mechanisms are present in metals as in semiconductors, but because of the large number of occupied states in the conduction bands of metals, the temperature dependences of the various scattering mechanisms are quite different.

9.3.1 Electron-Phonon Scattering in Metals

In metals as in semiconductors, the dominant scattering mechanism is usually electron-phonon scattering. In the case of metals, electron scattering is mainly associated with an electromagnetic interaction of ions with *nearby* electrons, the longer range interactions being **screened** by the numerous mobile electrons. For metals, we must therefore consider explicitly the probability that a state $\mathbf{k}$ is occupied $f_0(\mathbf{k})$ or unoccupied $[1 - f_0(\mathbf{k})]$. The scattering rate is found by explicit consideration of the scattering rate into a state $\mathbf{k}$ and the scattering out of that state. Using the same arguments as in Sect. 9.2.1, the collision term in Boltzmann's equation is given by

Table 9.1 Debye temperature of several metals

Symbol	Metal	Θ_D(K)
$\oplus$	Au	175
$\circ$	Na	202
$\triangle$	Cu	333
$\sqcap$	Al	395
$\bullet$	Ni	472

$$\left.\frac{\partial f}{\partial t}\right|_{\text{collisions}} \sim \frac{1}{\tau} \simeq \sum_q G(\mathbf{q}) \left\{ \overbrace{[1 - f_0(\mathbf{k})]\left[\underbrace{f_0(\mathbf{k}-\mathbf{q})n(\mathbf{q})}_{\text{phonon absorption}} + \underbrace{f_0(\mathbf{k}+\mathbf{q})[1+n(\mathbf{q})]}_{\text{phonon emission}} \right]}^{\text{scattering into } \mathbf{k}} \right. \\ \left. - \overbrace{[f_0(\mathbf{k})]\left[\underbrace{[1 - f_0(\mathbf{k}+\mathbf{q})]n(\mathbf{q})}_{\text{phonon absorption}} + \underbrace{[1 - f_0(\mathbf{k}-\mathbf{q})][1+n(\mathbf{q})]}_{\text{phonon emission}} \right]}^{\text{scattering out of } \mathbf{k}} \right\} \tag{9.43}$$

Here the first term in (9.43) is associated with scattering electrons into an element of phase space at $\mathbf{k}$ with a probability given by $[1 - f_0(\mathbf{k})]$ that state $\mathbf{k}$ is unoccupied and has contributions from both phonon absorption processes and phonon emission processes. The second term arises from electrons scattered out of state $\mathbf{k}$ and here, too, there are contributions from both phonon absorption processes and phonon emission processes. The equilibrium distribution function $f_0(\mathbf{k})$ for the electron is the Fermi distribution function while the function $n(\mathbf{q})$ for the phonons is the Bose distribution function (15.10). Phonon absorption depends on the phonon density $n(\mathbf{q})$, while phonon emission depends on the factor $\{1+n(\mathbf{q})\}$. These factors arise from the properties of the creation and annihilation operators for phonons (to be further discussed in the Problem set). The density of final states for metals is the density of states at the Fermi level which is consequently approximately independent of energy and temperature. In metals, the condition that electron scattering takes place to states near the Fermi level implies that the largest phonon wave vector in an electron collision is $2k_F$ where k_F is the electron wave vector at the Fermi surface.

Of particular interest is the temperature dependence of the phonon scattering mechanism in the limit of low and high temperatures. Experimentally, the temperature dependence of the resistivity of metals can be plotted on a universal curve (see Fig. 9.6) in terms of ρ_T/ρ_{Θ_D} vs. T/Θ_D where Θ_D is the Debye temperature. This plot includes data for several metals, and values for the Debye temperature of these metals are given with the figure (Table 9.1).

In accordance with the plot in Fig. 9.6, $T \ll \Theta_D$ defines the low temperature limit and $T \gg \Theta_D$ the high temperature limit. Except for the very low temperature

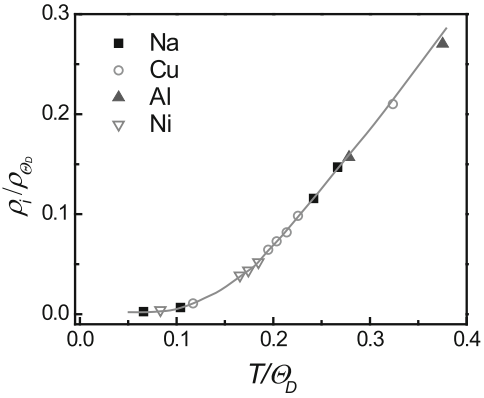

Fig. 9.6 Universal curve of the temperature dependence of the ideal resistivity of various metals normalized to the value at the Debye temperature as a function of the dimensionless temperature T/Θ_D

defect scattering limit, the electron-phonon scattering mechanism dominates, and the temperature dependence of the scattering rate depends on the product of the density of phonon states and the phonon occupation, since the electron-phonon coupling coefficient is essentially independent of T. The phonon concentration in the high temperature limit becomes

$$n(\mathbf{q}) = \frac{1}{\exp(\hbar\omega/k_B T) - 1} \approx \frac{k_B T}{\hbar\omega} \tag{9.44}$$

since $(\hbar\omega/k_B T) \ll 1$, so that from (9.44) we have $1/\tau \sim T$ and $\sigma = ne\mu \sim T^{-1}$. In this high temperature limit, the scattering is quasi-elastic and involves large-angle scattering, since phonon wave vectors up to the Debye wave vector q_D are involved in the electron scattering, where q_D is related to the Debye frequency ω_D and to the Debye temperature Θ_D according to

$$\hbar\omega_D = k_B\Theta_D = \hbar q_D v_q \tag{9.45}$$

where v_q is the velocity of sound.

We can interpret q_D as the radius of a Debye sphere in $\mathbf{k}$-space which defines the range of accessible $\mathbf{q}$ vectors for scattering, i.e., $0 < q < q_D$. The magnitude of wave vector q_D is comparable to the Brillouin zone dimensions but the energy change of an electron (ΔE) on scattering by a phonon will be less than $k_B\Theta_D \simeq 1/40eV$ so that the restriction of $(\Delta E)_{max} \simeq k_B\Theta_D$ implies that the maximum electronic energy change on scattering will be small compared with the Fermi energy E_F. We thus obtain that for $T > \Theta_D$ (the high temperature regime), $\Delta E < k_B T$ and the scattering will be quasi-elastic as illustrated in Fig. 9.7a.

In the opposite limit, $T \ll \Theta_D$, we have $\hbar\omega_q \simeq k_B T$ (because only low frequency acoustic phonons are available for scattering) and in the low temperature limit there is the possibility that $\Delta E > k_B T$, which implies inelastic scattering. In the low temperature limit, $T \ll \Theta_D$, the scattering is also small-angle scattering, since only

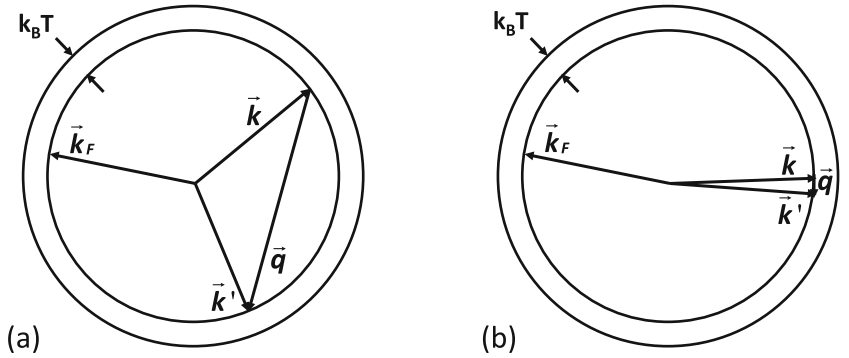

Fig. 9.7 **a** Scattering of electrons on the Fermi surface of a metal. Large angle scattering dominates at high temperature ($T > \Theta_D$) and this regime is called the "quasi-elastic" limit. **b** Small angle scattering is important at low temperature ($T < \Theta_D$) and is in general an inelastic scattering process

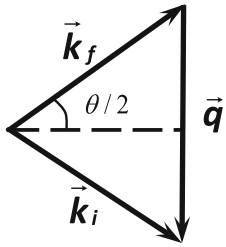

Fig. 9.8 Geometry of the scattering process, where θ is the scattering angle between the incident and scattered electron wave vectors $\mathbf{k}_i$ and $\mathbf{k}_f$, respectively, and q is the phonon wave vector

low energy (low q wave vector) phonons are available for scattering (as illustrated in Fig. 9.7b). At low temperature, the phonon density contributes a factor of T^3 to the scattering rate (9.43) when the sum over phonon states is converted to an integral and $q^2 dq$ is written in terms of the dimensionless variable $\hbar\omega_q / k_B T$ with $\omega = v_q q$. Since small momentum transfer gives rise to small angle scattering, the diagram in Fig. 9.8 involves Fig. 9.7. Because of the small energy transfer we can write,

$$|\mathbf{k_i} - \mathbf{k_f}| \sim k_f(1 - \cos\theta) \approx \frac{1}{2} k_f \theta^2 \approx \frac{1}{2} k_f (q/k_f)^2 \tag{9.46}$$

so that another factor of q^2 appears in the integration over $\mathbf{q}$ when calculating $(1/\tau_D)$. Thus, the electron scattering rate at low temperature is predicted to be proportional to T^5 so that $\sigma \sim T^{-5}$ (Bloch–Grüneisen formula). Thus, when phonon scattering is the dominant scattering mechanism in metals, the following results are obtained:

$$\sigma \sim \Theta_D / T \qquad T \gg \Theta_D \tag{9.47}$$

$$\sigma \sim (\Theta_D / T)^5 \qquad T \ll \Theta_D \tag{9.48}$$

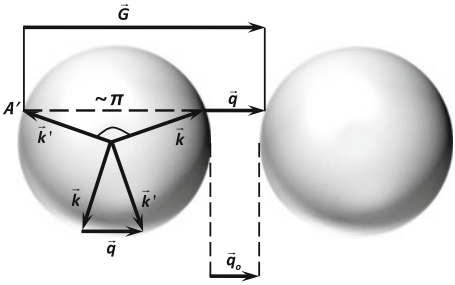

Fig. 9.9 Schematic diagram showing the relation between the phonon wave vector **q** and the electron wave vectors **k** and **k**′ in two Brillouin zones separated by the reciprocal lattice vector **G** (umklapp process)

In practice, the resistivity of metals at very low temperatures is dominated by other scattering mechanisms, such as impurities, boundary scattering, etc., and at very low T, electron-phonon scattering (see (9.48)) is relatively unimportant.

The possibility of *umklapp* processes further increases the range of phonon modes that can contribute to electron scattering in electron-phonon scattering processes. In an umklapp process, a non-vanishing reciprocal lattice vector can be involved in the momentum conservation relation, as shown in the schematic diagram of Fig. 9.9.

In this diagram, the relation between the wave vectors for the phonon and for the incident and scattered electrons $\mathbf{G} = \mathbf{k} + \mathbf{q} + \mathbf{k}'$ is shown when crystal momentum is conserved for a non-vanishing reciprocal lattice vector $\mathbf{G}$. Thus, phonons involved in an umklapp process have large wave vectors with magnitudes of about 1/3 of the Brillouin zone dimensions. Therefore, substantial energies can be transferred on collision through an umklapp process. At low temperatures, normal scattering processes (i.e., normal as distinguished from umklapp processes) play an important part in completing the return to equilibrium of an excited electron in a metal, while at high temperatures, umklapp processes become more important.

The discussion presented up to this point is applicable to the creation or absorption of a single phonon in a particular scattering event. Since the restoring forces for lattice vibrations in solids are not strictly harmonic, *anharmonic* corrections to the restoring forces give rise to *multiphonon* processes where more than one phonon can be created or annihilated in a single scattering event. Experimental evidence for multiphonon processes is provided in both optical and transport studies. In some cases, more than one phonon at the *same* frequency can be created (harmonics), while in other cases, multiple phonons at *different* frequencies (overtones and combination modes comprising phonons with two different frequencies) are involved.

9.3.2 *Other Scattering Mechanisms in Metals*

At very low temperatures where phonon scattering is of less importance, other scattering mechanisms become important, and we can write

$$\frac{1}{\tau} = \sum_i \frac{1}{\tau_i} \tag{9.49}$$

where the sum is over all the scattering processes, according to Matthiessen's rule.

(a) Charged impurity scattering — The effect of charged impurity scattering (Z being the difference in the charge on the impurity site as compared with the charge on a regular lattice site) is of less importance in metals than in semiconductors, because of the strong screening effects by the free electrons in metals.
(b) Neutral impurities — This process pertains to scattering centers having the same charge as the host. Such scattering has less effect on the transport properties than scattering by charged impurity sites, because of the much weaker scattering potential.
(c) Vacancies, interstitials, dislocations, size-dependent effects — the effects for these defects on the transport properties are similar to those for semiconductors. Boundary scattering can become very important in metal nanostructures when the sample length in some direction becomes less than the mean free path in the corresponding bulk crystal. In this case ballistic transport can occur by electrons that remain out of equilibrium until reaching the boundary of the sample.

For most metals, phonon scattering is relatively unimportant at liquid helium temperatures, so that resistivity measurements at 4 K provide one sensitive method for the detection of impurities and crystal defects. In fact, in characterizing the quality of a high purity metal sample, it is customary to specify the resistivity ratio $\rho(300\,\mathrm{K})/\rho(4\,\mathrm{K})$. This quantity is usually called the *residual resistivity ratio* (RRR), or the residual *resistance* ratio. In contrast, a typical semiconductor is characterized by its conductivity and Hall coefficient at room temperature and at 77 K.

9.4 Phonon Scattering

Whereas electron scattering is important in electronic transport properties, phonon scattering is important in thermal transport, particularly for the case of insulators where heat is carried mainly by phonons. The major scattering mechanisms for phonons are phonon-phonon scattering, phonon-boundary scattering, defect-phonon scattering, and phonon-electron scattering which are briefly discussed in the following subsections.

9.4.1 Phonon-Phonon Scattering

The dominant phonon scattering process in crystalline materials is usually phonon-phonon scattering. Phonons are scattered by other phonons because of anharmonic terms in the restoring potential. This scattering process permits:

- two phonons to combine to form a third phonon or
- one phonon to break up into two phonons.

In these anharmonic processes, energy and wavevector conservation apply:

$$\mathbf{q}_1 + \mathbf{q}_2 = \mathbf{q}_3 \qquad \text{normal processes} \tag{9.50}$$

or

$$\mathbf{q}_1 + \mathbf{q}_2 = \mathbf{q}_3 + \mathbf{Q} \qquad \text{umklapp processes} \tag{9.51}$$

where $\mathbf{Q}$ corresponds to a phonon wave vector of magnitude equal to a non-zero reciprocal lattice vector. Umklapp processes are important when q_1 or q_2 are large, i.e., comparable to a reciprocal lattice vector (see Fig. 9.10). When umklapp processes (see Fig. 9.10) are present, the scattered phonon wavevector $\mathbf{q}_3$ can be in a direction opposite to the energy flow, thereby giving rise to thermal resistance. Because of the high momentum transfer and the large phonon energies that are involved, *umklapp* processes dominate the thermal conductivity at high T.

The phonon density is proportional to the Bose factor so that the scattering rate is proportional to

$$\frac{1}{\tau_{\text{ph}}} \sim \frac{1}{(e^{\hbar\omega/(k_B T)} - 1)}. \tag{9.52}$$

At high temperatures $T \gg \Theta_D$, the scattering time thus varies as T^{-1} since

$$\tau_{\text{ph}} \sim (e^{\hbar\omega/k_B T} - 1) \sim \hbar\omega/k_B T \tag{9.53}$$

while at low temperatures $T \sim \Theta_D$, an exponential temperature dependence for τ_{ph} is found

$$\tau_{\text{ph}} \sim e^{\hbar\omega/k_B T} - 1. \tag{9.54}$$

These temperature dependences are important in considering the lattice contribution to the thermal conductivity (see Sect. 2.4).

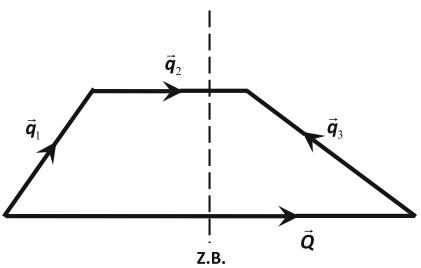

Fig. 9.10 Phonon-phonon umklapp processes. Here $\mathbf{Q}$ is a non-zero reciprocal lattice vector, and $\mathbf{q}_1$ and $\mathbf{q}_2$ are the incident phonon wavevectors involved in the scattering process, while $\mathbf{q}_3$ is the wavevector of the scattered phonon. The vertical dashed line denotes the Brillouin's zone boundary (Z.B.)

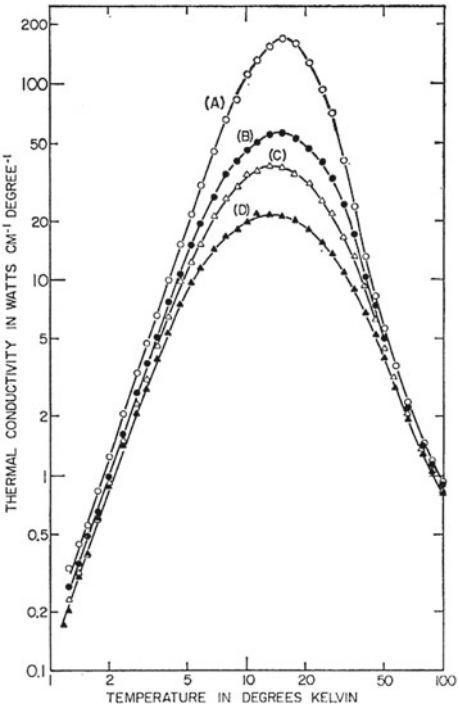

Fig. 9.11 For insulators, we often plot both the thermal conductivity κ and the temperature T on log scales. The various curves here are for LiF with different concentrations of Li isotopes ^{6}Li and ^{7}Li. For highly perfect crystals, it is possible to observe the scattering effects due to Li ions of different masses, which act as lattice defects but have little effect on the electronic properties. Reproduced with permission from Physical Review, vol. 156, pp. 975–988 Copyright (1967) American Physical Society

9.4.2 Phonon-Boundary Scattering

Phonon-boundary scattering is important at low temperatures where the phonon density is low. In this regime, the scattering time is independent of T. The thermal conductivity in this range is proportional to the phonon density which is in turn proportional to T^3. Phonon-boundary scattering is also very important for low dimensional systems where the sample size in some dimension is less than the corresponding phonon mean free path in the bulk 3D crystal. Phonon-boundary scattering combined with phonon-phonon scattering results in a thermal conductivity κ for insulators with the general shape shown in Fig. 9.11 (see Sect. 8.2.4). The lattice thermal conductivity follows the relation

$$\kappa_L = C_p v_q \Lambda_{\text{ph}}/3 \tag{9.55}$$

where the phonon mean free path Λ_{ph} is related to the phonon scattering probability $(1/\tau_{\text{ph}})$ by

$$\tau_{\text{ph}} = \Lambda_{\text{ph}}/v_q \tag{9.56}$$

in which v_q is the velocity of sound and C_p is the heat capacity at constant pressure. Phonon-boundary scattering becomes more important as the crystallite size

decreases. The scattering conditions at the boundary can be specular (where after scattering only $q_\perp$ is reversed and $q_\parallel$ is unchanged) for a very smooth sample surface, or the scattering conditions can be diffuse (where after scattering the q is randomized) for a rough sample surface. Periodic corrugations on a surface can also give rise to interesting scattering effects for both electrons and phonons.

9.4.3 Defect-Phonon Scattering

Defect-phonon scattering includes a variety of crystal defects, charged and uncharged impurities and different isotopes of the host constituents. The thermal conductivity curves in Fig. 9.11 show the scattering effects due to different isotopes of Li. The low mass of Li makes it possible to see such effects clearly. Isotope effects are also important in graphite and diamond which have the highest thermal conductivity of any solid, and also have several isotopes with large fractional mass differences between one another.

9.4.4 Electron-Phonon Scattering

If electrons scatter from phonons, the reverse process also occurs. When phonons impart momentum to electrons, the electron distribution is affected. Thus, the electrons will also carry energy as they are dragged also by the stream of phonons. This phenomenon is called *phonon drag*. In the case of phonon drag, we must simultaneously solve the Boltzmann equations for the electron and phonon distributions which are coupled by the phonon drag interaction term.

9.5 Temperature Dependence of the Electrical and Thermal Conductivity

For the electrical conductivity, at very low temperatures, impurity, defect, and boundary scattering dominate. In this regime σ is independent of temperature. At somewhat higher temperatures but still far below Θ_D the electrical conductivity for metals exhibits a strong temperature dependence (see (9.48))

$$\sigma \propto (\Theta_D/T)^5 \qquad T \ll \Theta_D. \tag{9.57}$$

At higher temperatures where $T \gg \Theta_D$, scattering by phonons with any q vector is possible and the formula

$$\sigma \sim (\Theta_D/T) \qquad T \gg \Theta_D \tag{9.58}$$

applies. We now summarize the corresponding temperature ranges for the thermal conductivity.

Although the thermal conductivity was formally discussed in Chap. 8, a meaningful discussion of the temperature dependence of κ involves scattering processes because of the different temperature dependence of the various scattering processes. The total thermal conductivity κ in general depends on the lattice and electronic contributions, κ_L and κ_e, respectively. The temperature dependence of the lattice contribution is discussed in Sect. 8.2.4 with regard to the various phonon scattering processes and their temperature dependence. For the electronic contribution, we must consider the temperature dependence of the electron scattering processes discussed in Sect. 9.2.

At very low temperatures, in the impurity/defect/boundary scattering range, σ is independent of T, and the same scattering processes apply for both the electronic thermal conductivity and the electrical conductivity, thus $\kappa_e \propto T$ in the impurity scattering regime where $\sigma \sim$ constant and the Wiedemann–Franz law is applicable. From Fig. 8.1 we see that for copper, defect and boundary scattering are dominant below ~20 K, while phonon scattering becomes important at higher T.

At low temperatures $T \ll \Theta_D$, but with T in a regime where phonon scattering has already become the dominant scattering mechanism, the thermal transport depends on the electron-phonon collision rate which in turn is proportional to the phonon density. At low temperatures the phonon density is proportional to T^3. This follows from the proportionality of the phonon density of states arising from the integration of $\int q^2 dq$. From the dispersion relation for the acoustic phonons $\omega = q v_q$ we obtain

$$\omega / v_q = x k T / \hbar v_q \tag{9.59}$$

where $x = \hbar\omega / k_B T$. Thus in the low temperature range of phonon scattering where $T \ll \Theta_D$ and the Wiedemann–Franz law is no longer satisfied, the temperature dependence of τ is found from the product $T(T^{-3})$ so that now $\kappa_e \propto T^{-2}$. One reason why the Wiedemann–Franz law is not satisfied in this temperature regime is that κ_e depends on the collision rate τ_c, while σ depends on the time to reach thermal equilibrium, τ_D. At low temperatures where only low q phonons participate in scattering events, the times τ_c and τ_D are not the same, and τ_D can be very long.

At high T where $T \gg \Theta_D$ and the Wiedemann–Franz law applies, κ_e approaches a constant value corresponding to the regime where σ is proportional to $1/T$. This occurs at temperatures much higher than those shown in Fig. 8.1. The decrease in κ above the peak value at ~17 K follows a $1/T^2$ dependence quite well.

In addition to the electronic thermal conductivity, heat can be carried by the lattice vibrations or phonons. The phonon thermal conductivity mechanism is in fact the principal mechanism operative in semiconductors and insulators, since the electronic contribution in this case is negligibly small. Since κ_L contributes also to metals, the total measured thermal conductivity for metals should exceed the electronic contribution $(\pi^2 k_B^2 T \sigma)/(3e^2)$. In good metallic conductors of high purity, the electronic thermal conductivity dominates and the phonon contribution tends to be small. On the other hand, in conductors where the thermal conductivity due

to phonons makes a significant contribution to the total thermal conductivity, it is necessary to separate the electronic and lattice contributions before applying the Wiedemann–Franz law to the total κ.

With regard to the lattice contribution, κ_L at very low temperatures is dominated by defect and boundary scattering processes. From the relation

$$\kappa_L = \frac{1}{3} C_p v_q \Lambda_{\text{ph}} \tag{9.60}$$

we can determine the temperature dependence of κ_L, since $C_p \sim T^3$ at low T, while the sound velocity v_q and phonon mean free path Λ_{ph} at very low T are independent of T. In this regime the number of scatterers is also independent of T.

In the regime where only low q phonons contribute to transport and to scattering, only normal scattering processes contribute. In this regime C_p is still increasing as T^3, v_q is independent of T, but $1/\Lambda_{\text{ph}}$ increases in proportion to the phonon density of states. With increasing T, the temperature dependence of C_p becomes less pronounced and that for Λ_{ph} becomes more pronounced as more scatters participate, leading eventually to a decrease in κ_L. We note that it is only the inelastic collisions that contribute to the decrease in Λ_{ph} and the inelastic collisions are of course due to anharmonic forces.

With increasing temperature, eventually phonons with wavevectors large enough to support umklapp processes are thermally activated. Umklapp processes give rise to thermal resistance and in this regime κ_L decreases as $\exp(-\Theta_{D/T})$. In the high temperature limit $T \gg \Theta_D$, the heat capacity and phonon velocity are both independent of T. Thus, the $\kappa_L \sim 1/T$ dependence arises from the $1/T$ dependence of the mean free path, since in this limit the scattering rate becomes proportional to $k_B T$.

Problems

9.1 By using simple physical arguments, demonstrate the relation given by (9.7).

$$\tau_D = \frac{\tau_c}{1 - \cos\theta} \tag{9.61}$$

9.2 The optical phonon energies of GaAs and AlAs are 36 and 50 meV, respectively, at the Brillouin zone center.

(a) What is the occupation probability of these optical phonons at 77 and 300 K?
(b) Estimate the relative importance of optical phonon absorption and phonon emission for scattering electrons in GaAs and AlAs at 100 K.
(c) Calculate the Debye temperature for GaAs where the sound velocity is 5.6×10^5 cm/s. Assume that the volume of the unit cell is $4.39 \times 10^{-23}\,\text{cm}^{-3}$.

9.3 In limiting the electrical transport in Si, the intervalley scattering is very important. In particular, two kinds of intervalley scatterings are important: in a g-scattering

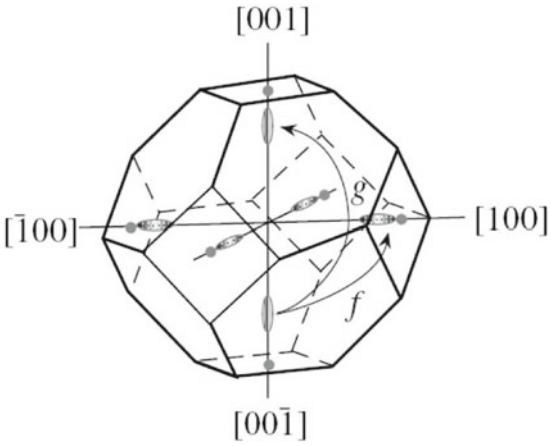

Fig. 9.12 Electron pockets in Si over the Brillouin zone. The schematic drawing highlights the g and f scattering processes listed in Sect. 9.2.3

event an electron goes from one valley (say a $(0,0,\Delta)$ valley) to an opposite valley $(0,0,-\Delta)$, while in an f-scattering event, the electron goes to a perpendicular valley ((00Δ) to $(0\Delta0)$, for example). The extra momentum for the transitions is provided by a phonon and may include a reciprocal lattice vector. Remember that Si valleys are not precisely at the X-point ($\Delta = 0.85$). The speed of sound in silicon is 8433 m/s.(See Fig. 9.12)

(a) Calculate the phonon wavevectors which allow these two scattering mechanisms to occur.
(b) Estimate the temperatures at which inter-valley scattering becomes important for electron conduction in Si, for both the g- and f-scattering mechanisms.

9.4 The phonon mean free path in bulk silicon is approximately $\lambda_{mfp} = 30$ nm at room temperature. This results in a lattice thermal conductivity of 1.38 W/cm·K, based on a heat capacity of C_v=1.66 J/K·cm^3 and a speed of sound v_g=8.3 $\times$ 10^5 cm/s. In silicon nanowires with diameters smaller than the bulk phonon mean free path, surface scattering can modify the phonon mean free path significantly. What is the lattice thermal conductivity of nanostructured silicon with a phonon mean free path of 10 nm?

9.5 Bi_2Te_3 has a lattice thermal conductivity of 1.5 W/m·K, heat capacity of 1.2×10^6 J/K·m^3, and speed of sound $v_g = 3 \times 10^3$ m/s. Based on these values, what is the approximate size of a Bi_2Te_3 nanostructure (i.e., nanowire) below which a substantial reduction in the thermal conductivity can be achieved through surface phonon scattering?

9.6 Isotopic doping can be used to increase the scattering of phonons in crystalline materials. Consider three graphite samples prepared with 1.1% ^{13}C (natural abundance), 50% ^{13}C, and 99% ^{13}C. Of these samples, which material has the lowest thermal conductivity? Explain why.

9.7 What is the minimum electron energy that is needed to create a 50 meV phonon of maximum wave vector (from the zone center to the zone boundary) in a semiconductor with the diamond structure where the nearest neighbor distance is 2 Å?

9.8 (a) Assuming a 1D carrier concentration of 10^6 electrons/cm, how many conduction electrons are contained per cm^3 in a quantum wire if $a = 25$ Å?
(b) Suppose that you have a Si sample and you would like to know the temperature below which defect scattering dominates over the intrinsic phonon scattering, how would you proceed?
(c) How would you distinguish between the relative importance between phonon absorption and phonon emission processes for scattering electrons in an electrical conductivity measurement in the 70–80 K temperature range in a high quality Si sample with few defects, other than the dopants used to generate the electron carrier concentration in making the sample *n*–type?

9.9 Why is optical phonon scattering not important for electron transport in copper?

9.10 Estimate the relative importance of phonon absorption to phonon emission for scattering electrons in an intrinsic GaAs sample at 100 K.

Suggested Readings

Ashcroft, Mermin, *Solid State Physics* (Holt, Rinehart and Winston, New York, 1976). Chapters 16 and 26
G. Chen, M.S. Dresselhaus, G. Dresselhaus, J.P. Fleurial, T. Caillat, Recent developments in thermoelectric materials. Int. Mater. Rev. **48**, 45–66 (2003)
Hang, *Theoretical Solid State Physics*, vol. 2 (Pergamon, New York, 1972). Chapter 4
C. Kittel, *Introduction to Solid State Physics*, 6th edn. (Wiley, New York, 1986). Appendix C
S. Link, M.A. El-Sayed, Spectral properties and relaxation dynamics of surface plasmon electronic oscillations in gold and silver nanodots and nanorods. Phys. Chem. B **103**, 8410–8426 (1999)
M. Lundstrom, *Fundamentals of Carrier Transport* (Cambridge University Press, Cambridge, 2000)